SMIREP: Predicting Chemical Activity from SMILES

Andreas Karwath* and Luc De Raedt

Institut für Informatik, Albert-Ludwigs Universität Freiburg, Georges-Köhler-Allee 079,
D-79110 Freiburg, Germany

Received May 2, 2006

Most approaches to structure−activity-relationship (SAR) prediction proceed in two steps. In the first step, a typically large set of fingerprints, or fragments of interest, is constructed (either by hand or by some recent data mining techniques). In the second step, machine learning techniques are applied to obtain a predictive model. The result is often not only a highly accurate but also hard to interpret model. In this paper, we demonstrate the capabilities of a novel SAR algorithm, SMIREP, which tightly integrates the fragment and model generation steps and which yields simple models in the form of a small set of IF-THEN rules. These rules contain SMILES fragments, which are easy to understand to the computational chemist. SMIREP combines ideas from the well-known IREP rule learner with a novel fragmentation algorithm for SMILES strings. SMIREP has been evaluated on three problems: the prediction of binding activities for the estrogen receptor (Environmental Protection Agency's (EPA's) Distributed Structure-Searchable Toxicity (DSSTox) National Center for Toxicological Research estrogen receptor (NCTRER) Database), the prediction of mutagenicity using the carcinogenic potency database (CPDB), and the prediction of biodegradability on a subset of the *Environmental Fate Database* (EFDB). In these applications, SMIREP has the advantage of producing easily interpretable rules while having predictive accuracies that are comparable to those of alternative state-of-the-art techniques.

1. INTRODUCTION

In the past few decades, a number of computational methods to predict structure−activity relationships (SAR) or quantitative structure−activity relationships (QSAR) based on 2D or 3D models of molecules have have been proposed for fast high-throughput screening. Most of these approaches assume that the relevant fragments, biophores, or fingerprints are provided by an expert or are calculated apriori and then induce a predictive model employing these. The commonly used MDL key sets[1,2] can be seen as an example of these predefined fragments or fingerprint approach. It is also possible to employ a number of other structural, topological, or physiochemical descriptors calculated by specialized software such as Molconn-Z[3] and use them for high-throughput screening of larger databases. However, as the generation of the relevant structural alerts or fragments is a nontrivial task, which greatly determines the quality of the learned model, several recent approaches from the field of data mining try to automate this generation process.

First, a number of graph-mining methods have been employed to SAR problems in order to discover the necessary relevant fragments. The vast majority of these approaches computes fragments (sometimes called local patterns) that frequently occur in or are significant with respect to a given data set, cf. Dehaspe,[4] Deshpande et al.,[5] Kramer et al.,[6,7] Zaki,[8] Yan and Han,[9] Borgelt and Berthold,[10] Inokuchi et al.,[11,12] and Kuramochi and Karypis.[13] The earliest approaches[4] to compute such fragments are based on techniques from inductive logic programming (ILP).[14] Whereas ILP techniques are theoretically appealing because of the use of expressive representation languages, they exhibit significant efficiency problems, which in turn implies that their application has been restricted to finding relatively small fragments in relatively small databases. Recently proposed approaches to mining frequent fragments in graphs such as gSpan,[9] CloseGraph,[15] FSG,[5] MoFa,[10] Gaston,[16] and AGM[12] are able to mine complex subgraphs more efficiently. However, the key difficulty with the application of these techniques is—as for other frequent pattern mining approaches—the number of patterns that are generated. For instance, Inokuchi et al.[11] report on the order of 10^6 patterns being discovered. Furthermore, frequent fragments are not necessarily of interest to a molecular scientist. Therefore, Kramer et al.[6] and Inokuchi and Kashima[11] take into account the classes of the molecules. Kramer et al. compute all simple patterns that are frequent in the actives and infrequent in the inactives, whereas Inokuchi et al. compute correlated patterns.

Second, there exist a few approaches that integrate the discovery of the fragments with the learning of the predictive model, most notably the CASE/MULTICASE family[17,18] and the more recent LAZAR system by Helma.[19] For instance, the well-known MULTICASE system constructs fixed sized fragments from the compounds and then uses a divide-and-conquer strategy (based on statistical tests) to distinguish between major biophores for classification and modulators that can regulate activity of a primary biophore as well as for biophobes indicating inactivity. The generated biophores or fragments are in principle linear fragments (though MULTICASE also supports branches around the backbone) and, hence, do not necessarily capture more complex

* Corresponding author phone: +49 761 203 8029; e-mail: karwath@informatik.uni-freiburg.de.

10.1021/ci060159g CCC: $33.50
Published on Web 10/12/2006

structures of chemical compounds. Furthermore, it is hard to find detailed information about the way the fragments are generated. The recent LAZAR approach by Helma[19] identifies linear fragments present in a compound database, identifies the relevant ones (using a statistical test), removes redundant ones, and predicts activity or inactivity for a given test compound based on majority vote. Similar to MULTICASE, the employed fragments are linear and include more complex structures, such as rings, only indirectly within their predictions. Furthermore, MULTICASE and LAZAR employ a weighting/scoring scheme on the fragments to make predictions, which are not always easy to understand or interpret.

The approach employed in SMIREP[20] is different. SMIREP combines the chemical modeling language SMILES (Simplified Molecular Input Line Entry System,[21] with IREP (Incremental Reduced Error Pruning), a state-of-the-art machine learning algorithm that produces a predictive model in the form of a small set of IF-THEN rules. It is essentially a specialized learning system for SAR and QSAR applications and for fast extraction of relevant structural fingerprints or features. In SMIREP, each IF-THEN rule lists one or more fragments that must be present in order for a compound to be active and, hence, describes directly a structural alert that is easy to interpret. The generation of the fragments is performed directly on the SMILES representations of the compounds and is guided by heuristics from the well-known rule-learner IREP.[22,23] We have applied SMIREP to three SAR problems: the prediction of binding activities for the estrogen receptor (EPA's DSSTox NCTRER Database), the prediction of mutagenicity using the carcinogenic potency database (CPDB), and the prediction of biodegradability on a subset of the Environmental Fate Database (EFDB). The experiments show that SMIREP produces *small* rule sets containing possibly *complex* fragments, that SMIREP is competitive in terms of predictive accuracy, and that SMIREP is quite efficient as compared to alternative methods.

2. METHODS

2.1. Databases. DSSTox NCTRER. The estrogen database was extracted from the EPA's DSSTox NCTRER Database (http://www.epa.gov/nheerl/dsstox/sdf_nctrer.html). The original data set was published by Fang et al.[24] and is specially designed to evaluate QSAR approaches. The NCTRER database provides activity classifications for a total of 232 chemical compounds, which have been tested regarding their binding activities for the estrogen receptor. The database contains a diverse set of natural, synthetic, and environmental estrogens and is considered to cover most known estrogenic classes spanning a wide range of biological activity.[24]

The database distributed by the EPA's DSSTox is in SDF (Structure Data Format) and contains, in addition to the original database, a number of annotations: 6 indicator variables extracted from the original publication,[24] logP (octanol/water partition coefficient) values, and chemical class assignments (6 main classes, 20 subclasses) as well as the activity category ER-RBA (estrogen receptor relative binding affinity). This classification yields 131 active and 101 inactive compounds (with regard to their ER-RBA).

CPDB. The original carcinogenic potency database (CPDB: http://potency.berkeley.edu/cpdb.html) provides carcinogenic as well as mutagenic classifications as determined by the *Salmonella*/microassay for a number of chemical compounds mainly of industrial and pharmaceutical interest. The database employed here was published by Helma et al.,[7] filtered to eliminate mixtures and undefined structures, and annotated with SMILES strings for each compound. The filtered database was downloaded from http://www.predictive-toxicology.org/data/cpdb_mutagens/.

Overall, the database contains 684 chemical structures (341 mutagens and 343 non-mutagens). Each entry is annotated with a variety of precalculated numerical attributes as well as other relevant information such as logP, homo, lumo, electronegativity, and other numerical properties.

EFDB. This database originates from a study about biodegradability of a number of commercially available chemical compounds. The data set was first published by Howard et al.[25] and has been used to evaluate the prediction capabilities of a number of relational classifications methods,[26,27] where a subset of 328 chemicals was used. We have selected this data set to be able to compare SMIREP's performance to some other state-of-the-art approaches from the machine learning and data-mining community. The data sets main source is the *Syracuse Research Cooperation's* (SRC) *Environmental Fate Database* (EFDB). The database contains degradation rates (in form of half-life times) for chemicals, considering *biotic*, *abiotic*, and *all* degradation within four environmental situations (soil, air, surface water, and groundwater). Furthermore, these degradation rates are measured within three environmental conditions *aerobic*, *anaerobic*, and *removal in wastewater treatment plants*. To be able to compare our approach to previously published work,[26,27] we restrict ourselves to the aqueous biodegradation in aerobic conditions. We use the same procedure of dividing the chemicals into degradable and nondegradable as Blockeel et al.[27] That is, compounds considered to degrade are compounds possessing half-life times of up to 4 weeks, or they are considered nondegradable otherwise. In addition to the 2D structure of the chemicals, global attributes are available like logP and the compound's molecular weight.

2.2. SMILES and SMARTS. SMILES. SMILES[21] is a well-known linear string representation language for chemical molecules. The SMILES language is commonly used in computational chemistry and is supported by the major software tools in the field, such as the commercial Daylight toolkit and the Open-Source OpenBabel library.

The SMILES notation of chemical compounds is comprised of atoms, bonds, parentheses, and numbers. Atoms are represented by their atomic symbols. The four basic bond types are represented by the symbols '-', '=', '#', and ':'. Ionic bonds, or *disconnections*, are represented by a '.'. Branches are specified by enclosing brackets, "(" and ")". Cyclic structures are represented by breaking one bond in each ring. The atoms adjacent to the bond obtain the same number. Here, we refer to these numbers as *cyclic link numbers*. The cyclic link numbers are not necessarily unique within a SMILES representation of a molecule.

To search for subgraphs in compounds encoded in SMILES, one can use the SMARTS language.[28] While SMILES is a language representing molecules, SMARTS is a language representing SMILES fragments. Although

SMARTS allows the use of wildcards and more complicated constraints, SMIREP uses only the SMILES subset of the SMARTS pattern language, that is, we use the SMILES notation for fragments.

Chirality. As the SMIREP approach presented in this work is very much database driven, we have examined the databases used for occurrences of stereoisomers with different activities. We have done this by comparing the main layer of the InChI codes[29] of all molecules (generated with the InChI generation tool downloaded from http://www.iupac.org). This allows one to detect molecules having the same skeletons and atomic composition as well as stereoisomers.

In the DSSTox NCTRER data set, only five compounds have a R/S complement, and only one compound has stereoisomers with different activities. Similarly, in the CPDB data set, we found only one pair of compounds possessing the same skeleton and atomic composition but having assigned different activities. In the EFDB we found no compounds possessing the same skeleton while being classified in different categories. This information is insufficient for discovering chirality dependent rules. Therefore, we have chosen to explicitly disregard chirality information in all compounds in the three databases.

2.3. SMIREP. Setting. SMIREP[20] aims at automatically discovering fragments, alerts, or biophores that discriminate the active compounds from the inactive ones. The discovered fragments are incorporated into IF-THEN rules, which essentially test whether a set of fragments is all present. When *all* fragments stated in the IF part of a rule are present in a compound, we also say that the rule *covers* the compound. For instance, consider the following two rules:

```
IF a compound contains the fragments:

       'cccc' AND 'ccN' AND 'ccO' AND 'OC'

THEN the compund is active

IF a compound contains the substructures:

       'c1ccccc1' AND 'Nccc'

THEN the compund is active
```

These rules are conjunctive and contain SMARTS patterns as their conditions. Furthermore, together they constitute to a rule-set, which is a predictive model that is used for classifying compounds as follows: if there is a rule that covers the compound, then predict "active"; otherwise predict "inactive". The rules are evaluated in SMIREP using the OpenBabel toolkit (www.openbabel.org) and are also easy to interpret as one classifies on the basis of the presence (or absence) of certain fragments. An actual rule set computed by SMIREP can be found in Table 3.

The problem tackled by SMIREP can now be formulated as follows:

Given: a set of compounds in SMILES format, where each compound is classified as either ***active*** or ***inactive***

Find: a rule-set that accurately discriminates *active* from *inactive* compounds.

Table 1. Confusion Matrix with Four Possible Outcomes: TP, TN, FP, and FN[a]

	predicted	
	active	inactive
active	TP	FP
inactive	FN	TN

[a] TP denotes the number of true positives, and TN denotes the number of true negatives. The number of errors made by predicting a compound of being active while it is not is denoted by FP (false positives), while predicting a compound to be inactive while it is active is denoted by FN (false negatives).

Table 2. Accuracy and Area Under ROC Curve for the NCTRER ER-Binding Data Set for the Different Settings and Beamsizes (k) from the 10 × 10-Fold Cross-Validations[a]

setting	k	acc training	AUC training	acc testing	AUC testing
SAR	5	80.34 (0.41)	0.832 (0.021)	78.96 (1.13)	0.816 (0.087)
	10	80.13 (0.51)	0.830 (0.021)	78.49 (1.92)	0.810 (0.077)
	20	80.05 (0.29)	0.826 (0.018)	77.62 (1.56)	0.800 (0.098)
QSAR	5	80.68 (0.63)	0.833 (0.024)	76.98 (1.41)	0.795 (0.090)
	10	80.68 (0.47)	0.831 (0.026)	77.69 (2.33)	0.802 (0.098)
	20	80.83 (0.45)	0.834 (0.022)	78.17 (1.90)	0.806 (0.074)

[a] The numbers in brackets denote the standard deviation. Surprisingly, the predictive performance drops slightly when numerical attributes are used in this experiment. A similar effect has also been reported by Helma et al.[7] on a different data set. Although, we have used a bin size of five to avoid overfitting, it still seems that in this experiment SMIREP does overfit slightly. An indicator for this is the difference in the training accuracy when compared to the testing accuracy. The training accuracy in the QSAR setting is always higher than the one for the SAR setting. However, the testing accuracy shows a higher drop as in the SAR setting.

As the discovered rule set should be used for classification, SMIREP searches for rules that satisfy many of the actives and few of the inactive ones. The task of finding rule sets for classification has been well-studied in the field of machine learning.[22,30,31] The key difference with traditional rule-set learning problems in machine learning lies in the use of the SMILES and SMARTS languages for representing compounds and patterns. SMIREP embraces several ideas from a well-known rule-learner from the field of machine learning, IREP,[22,23] but was adapted for the use of SMILES and SMARTS as representation languages.

In a previous preliminary publication,[20] we have introduced SMIREP in a computer science context demonstrating SMIREP's ability to tackle activity predictions within large databases of chemical compounds. The work presented here concentrates on the applicability and performance of SMIREP within a number of chemical applications.

Overview. SMIREP follows essentially a separate-and-conquer approach,[32] in which one iteratively searches for a single rule that covers many of the active compounds and none (or only very few) of the inactive ones. Once such a rule is found, it is added to the rule set, and the actives covered by the found rule are deleted. This process is then repeated until further rules do not yield any improvement with regard to a scoring function or all actives have been covered. The main SMIREP algorithm is depicted in Algorithm 1 (see Chart 1).

In order to search for one rule, SMIREP employs a so-called *seed compound*. The SMILES representation of the seed compound is decomposed in a *fragment tree*, which then determines the possible steps taken through the search space by the refinement operators (see section 2.3.4). To

Table 3. Example Rule Set Induced by SMIREP on the NCTRER ER-Binding Database[a]

No	Rules	Description
1	ccccO ∧ C(c1ccccc1)(C)C 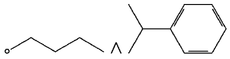	This rule seems to be be related to the Fang *et al.* rule set by enforcing the presence of an aromatic ring structure, as well as the presence of an oxygen attached to an aromatic ring structure (first part of the rule). Overall this rule also implies a certain hydrophobicity due to the large amount of aromatic bonds.
2	CCCCCCc1ccccc1 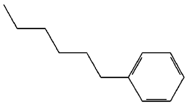	This rule seems to imply a certain size and hydrophobicity of the molecule but no precise information about the required H-bonding capabilities. In fact this rule covers only a fraction of features which active ER-binding substances should possess.
3	c1c(occ2ccc(cc2)O)cccc1 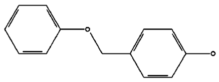	The rule depicts a 2D chemical structure similar to the DES skeleton used in Hong *et al.*,[39] and describes an aromatic ring connected to a phenolic ring structure by two atoms, oxygen and carbon via aromatic bonds. This is not exactly the DES skeleton, as firstly the bonds are not variable and secondly not both atoms are carbons.
4	Occ ∧ C=Ccccc 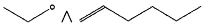	This rule does not correspond to any rule in the Fang *et al.* rules. The two facts correspond to some particular parts of those rules: the *Occ* fragment implies the presence of at least one of two required H-bonding sites, while the *C=Ccccc* fragment implies some larger aromatic structures, especially in combination with the first fragment.
5	Cc1ccc(cc1)O 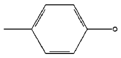	Rule 5 as well as rules 6 capture the existence of an phenolic ring structure within a compound, that matches some part of the rule system by Fang *et al.*
6	ccc1ccc(cc1)O 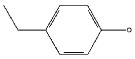	
7	Occcc ∧ CCCO 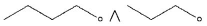	This rule is similar to rule 4. In addition to the two features noted above, this rule implies two OH groups instead of one, separated by a relatively long chain - or even one ore more rings, partly aromatic and partly non-aromatic.

[a] The description compares these rules to the rule set published by Fang et al.[24]

avoid being only dependent on one single compound while searching for rules, various randomly selected seeds are considered in the construction process. The search process for a single rule is composed of two steps: growing and

Chart 1. Algorithm 1: SMIREP

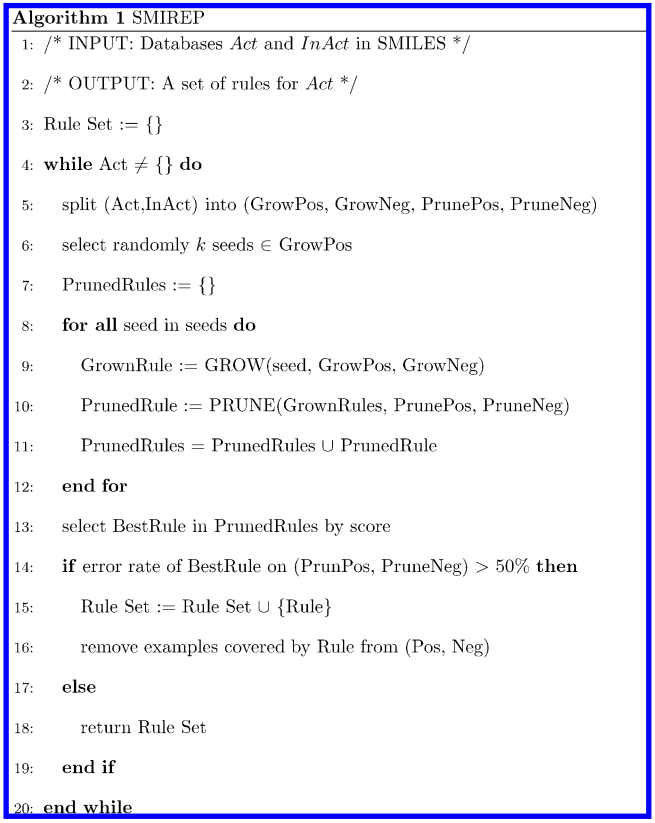

```
Algorithm 1 SMIREP
/* INPUT: Databases $Act$ and $InAct$ in SMILES */
/* OUTPUT: A set of rules for $Act$ */
Rule Set := {}
while Act $\neq$ {} do
    split (Act,InAct) into (GrowPos, GrowNeg, PrunePos, PruneNeg)
    select randomly $k$ seeds $\in$ GrowPos
    PrunedRules := {}
    for all seed in seeds do
        GrownRule := GROW(seed, GrowPos, GrowNeg)
        PrunedRule := PRUNE(GrownRules, PrunePos, PruneNeg)
        PrunedRules = PrunedRules $\cup$ PrunedRule
    end for
    select BestRule in PrunedRules by score
    if error rate of BestRule on (PrunPos, PruneNeg) $>$ 50% then
        Rule Set := Rule Set $\cup$ {Rule}
        remove examples covered by Rule from (Pos, Neg)
    else
        return Rule Set
    end if
end while
```

pruning, which employ different partitions of the training set. Indeed, the original data set is randomly divided into a growing and a pruning set. This division is done using a 2:1 split, i.e., two-thirds for growing a rule and one-third for pruning the rule.

Seeds and Fragments. While searching for a single rule, SMIREP employs the *fragment tree* of a seed compound to guide the search through the space of potential rules. The fragment tree is obtained by syntactically decomposing the SMILES representation of the compound and all growing and pruning operations employ this fragment tree. Furthermore, all rules evaluated (starting from a particular seed) will also cover that seed.

To obtain the fragment tree, SMIREP splits a SMILES string into cyclic fragments and branching fragments. Branching fragments are extracted from a SMILES string as follows: given a SMILES string of the form $A(B)C$, find the first branch, denoted by opening and corresponding closing brackets. The substring ranging from the start of the string to the opening branch is defined as fragment A with label a, the branch itself as fragment B with label b, and the rest after the branch as fragment C with label c (cf. Figure 1). Each B and C fragment can contain further branches. This splitting is applied recursively, until no more branches can be found. Note that we neither use a unique SMILES representation nor a canonical form, when fragmenting the SMILES strings. However, as the fragments are later on evaluated using the OpenBabel toolkit's SMARTS matching feature, any equivalent SMILES fragment would match a given compound.

Cyclic fragments are extracted in order to be able to represent ring structures and other types of cyclic structures. To ease the parsing of the string, each cycle number in the SMILES string is first assigned a unique value, as the SMILES language allows the 'reuse' of cycle numbers. To split a string into cyclic fragments, we extract the substrings within the corresponding numbers. The fragments are 'cleaned' before testing their coverage on the database, i.e., other link numbers not denoting a full ring are removed as well as redundant opening or closing brackets. Examples of cyclic fragments are shown in Figure 1 colored in blue. Like the branching fragments, the extraction of cyclic fragments is done recursively.

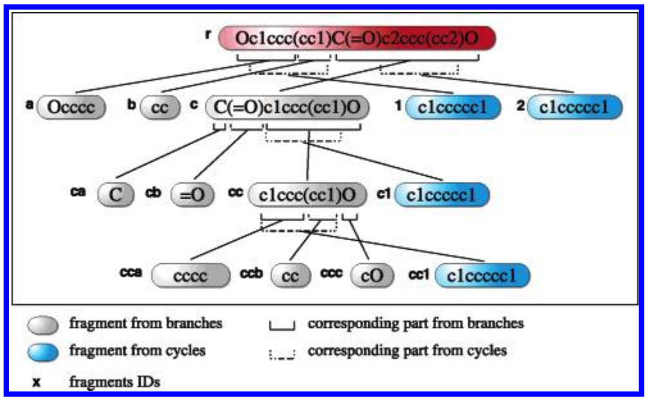

Figure 1. An example fragment tree of 4,4′-dihydoxybenzophenone. The original SMILES string for this molecule is *Oc1ccc(cc1)C(=O)c2ccc(cc2)O*, which is shown at the top of the tree. The first three fragments in the second line (colored gray) result from the branching decomposition, the other ones (colored blue) from the cycle identification. After the first decomposition, only one fragment can further be decomposed, namely the fragment with ID **c** shown in the third level of the tree. Again only the fragment with ID **cc** can be decomposed further, resulting in the final level of the tree. After the last decomposition, no more fragments can be generated. The leaves of the tree, namely fragments **a, b, 1, 2, ca, cb, c1, cca, ccb, ccc,** and **cc1** are the so-called ground fragments. Please note that the IDs last character denotes the label of the fragment. The IDs given here are purely used for clarity; they are neither constructed nor used in SMIREP.

Please note that not all possible rings in a compound can be found this way. For instance, if a compound's SMILES representation contains S = "c12ocnc2cccc1", the fragment decomposition will only extract one fragment containing both rings (CF_1 = "c12ocnc2cccc1") and one containing the inner ring alone (CF_2 = "c1ocnc1"). [Here, "inner ring" is used in the sense that one ring is within the other in the SMILES representation.]

The cyclic and branching fragments found in the above way form a tree, a so-called *fragment tree*. The leaves in the tree are fragments, which cannot be decomposed any further. We call these fragments *ground fragments*. Figure 1 shows such a tree for a small example compound.

Growing. For each of the growing iterations, SMIREP first selects a seed example, computes the corresponding fragment tree, and learns a rule as follows. First, the algorithm uses each ground fragment as an initial rule and evaluates it on the data set. The top k most promising rules (where k is a positive integer) are selected for the next refinement iteration. The parameter k is later on referred to as the *beamsize*.

The scoring heuristic used in SMIREP is weighted information gain (WIG), as originally suggested by Fürnkranz.[22] It is defined as follows[33]

$$\mathrm{WIG}(r) = -p(r)(\mathrm{IC}(r) - \mathrm{IC}(r'))$$

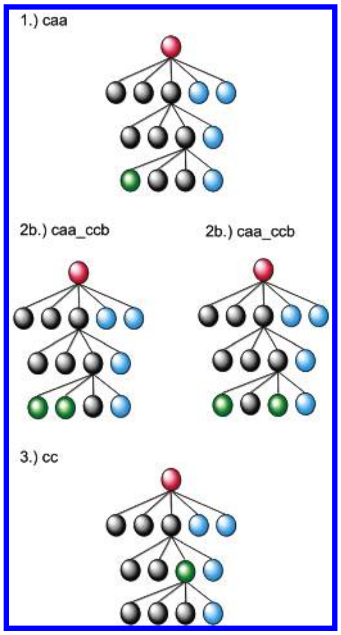

Figure 2. A hypothetical refinement example trace of an *Ascending* refinement, reflecting the example fragment tree in Figure 1. The green nodes correspond to the fragment or combined fragment evaluated during the *Ascending* refinement. Assume that the fragment **cca** is interesting according to the scoring function. Possible refinements would be combining fragment **cca** with **ccb**, resulting in a fragment **cca_ccb**. If either of the two new fragments receive a good score, the next refinement is to combine all three fragments **cca_ccb_ccc**, which is actually the same as fragment **cc**, which is then the next one to be evaluated.

where *p*(*x*) denotes the number of active examples covered by the rule *x*, IC(*x*) denotes the information content of a rule *x*, *r* denotes the current rule, and *r*′ denotes the predecessor of current rule, i.e., the current rule before the last refinement. The information content (IC) is defined as

$$\mathrm{IC}(x) = -\log\frac{p(x)}{p(x) + n(x)}$$

where *p*(*x*) denotes the number of active examples covered by rule *x*, and *n*(*x*) denotes the number of inactive examples covered by rule *x*. For the WIG measure, the difference in the information content of a rule and the same rule after refinement is weighted by the number of covered active examples.

Like many machine learning algorithms, SMIREP uses a *refinement operator*. A refinement operator essentially generalizes or specializes an existing rule or pattern. The refinement operator used in SMIREP is defined in Figure 3. In principle, refinement proceeds in a bottom-up manner, i.e., specializing a rule each time the operator is employed. In SMIREP new rules are constructed by either combining corresponding fragments from the tree (*Ascending*) or by adding new fragments to an existing rule (*Lengthening*).

While the *Ascending* refinement operator allows only to learn rules based on the fragments siblings and parents, the *Lengthening* refinement operator allows more complex rules to be learned. The *Lengthening* refinement operator allows the addition of new fragments to an existing rule. Consider the example where fragment **cc** (taken from the example fragment tree in Figure 1) does not perform better than **cca_ccb**. Fragment **cc** is therefore not further refined using the *Ascending* operator. However, combining it with another ground fragment might potentially perform better than the fragment itself. Therefore the *Lengthening* refinement can add new fragments (in the form of ground fragments) to an existing rule. The meaning of such a composite rule is that both fragments have to occur simultaneously within a compound to be classified as active.

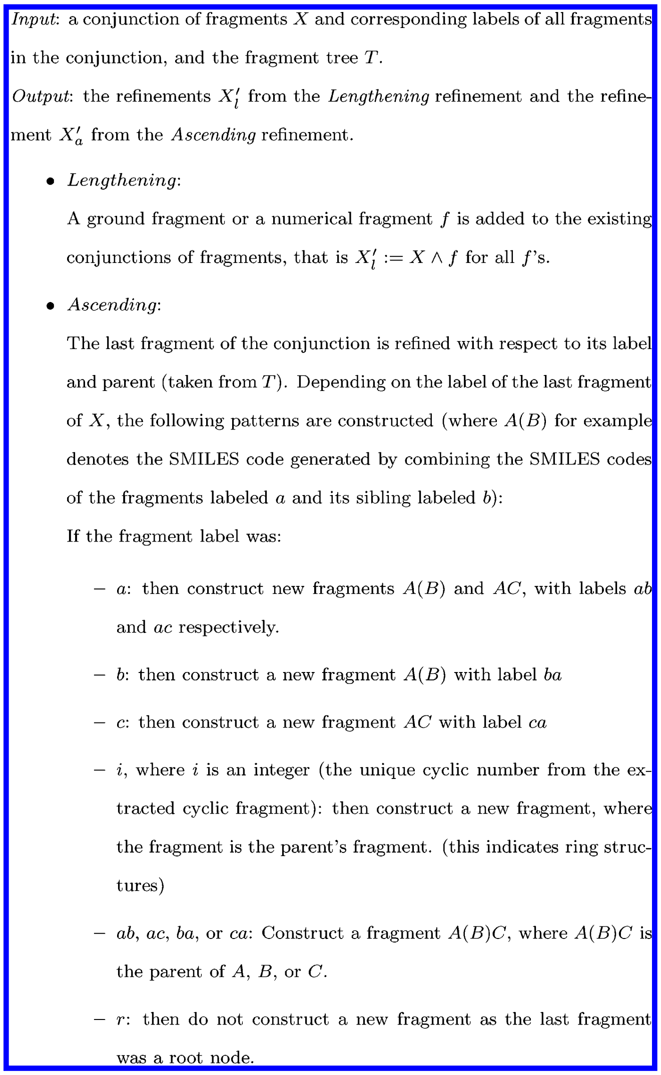

Input: a conjunction of fragments X and corresponding labels of all fragments in the conjunction, and the fragment tree T.

Output: the refinements X'_l from the *Lengthening* refinement and the refinement X'_a from the *Ascending* refinement.

- *Lengthening*:

  A ground fragment or a numerical fragment f is added to the existing conjunctions of fragments, that is $X'_l := X \wedge f$ for all f's.

- *Ascending*:

  The last fragment of the conjunction is refined with respect to its label and parent (taken from T). Depending on the label of the last fragment of X, the following patterns are constructed (where $A(B)$ for example denotes the SMILES code generated by combining the SMILES codes of the fragments labeled a and its sibling labeled b):

  If the fragment label was:

  – a: then construct new fragments $A(B)$ and AC, with labels ab and ac respectively.

  – b: then construct a new fragment $A(B)$ with label ba

  – c: then construct a new fragment AC with label ca

  – i, where i is an integer (the unique cyclic number from the extracted cyclic fragment): then construct a new fragment, where the fragment is the parent's fragment. (this indicates ring structures)

  – ab, ac, ba, or ca: Construct a fragment $A(B)C$, where $A(B)C$ is the parent of A, B, or C.

  – r: then do not construct a new fragment as the last fragment was a root node.

Figure 3. The refinement operator used in SMIREP. In each iteration of the algorithm, both refinements of the operator can be applied. During the search, the rule with the best *score* (see text) is selected. Please note, that in the ascending part of the operator, no construction of a new fragment labeled *b* and *c* alone is performed, as both fragments rely on an atom and bond from fragment labeled *a*. Consider the fragment *C(Cl)Cl*, with subfragments **a** = *C*, **b** = *Cl*, and **c** = *Cl*. Combining **b** and **c** would require the carbon atom *C* from fragment **a**.

Furthermore, SMIREP allows the use of numerical attributes. This has been incorporated in the algorithm by generating new types of fragments, *numerical fragments*, denoting that a particular numerical attribute is *less than* or *greater or equal to* some numerical value. Only those values which are true on the current seed are considered. These fragments can only be added during the *Lengthening* refinement of the growing stage. By adding more than one numerical constraint using the same attribute, it is possible for SMIREP to use intervals, i.e., it is possible to have rules containing the following constraint: ‘logP > −1.11’ ∧ ‘logP ≤ 3.21’. These numerical constraints allow SMIREP to be used in the quantitative structure–activity relationships (QSAR) setting. To avoid overfitting, SMIREP first discretizes the numerical attributes into equal frequency bins. During each iteration of the growing stage, all borders of these bins are dynamically evaluated on the current growing set, and the borders are added as new attributes. If a particular seed possesses a *logP* value of 3.24, and the binning resulted in the four borders $B_s = [0.33, 2.66, 4.99, 7.32]$, then the following attributes are evaluated: 'logP > 0.33', 'logP > 2.66', 'logP ≤ 4.99,' and 'logP ≤ 7.32'. The number of bins used in this work has arbitrarily been set to five.

Pruning. To avoid overfitting of the rules learned in the growing stage of the algorithm, the rules are pruned using the pruning set. The pruning is performed in reverse order of the growing of rules, i.e., the refinements are "undone". To this aim, the actual refinement history is stored for each rule. All rules resulting from this reverse refinement are evaluated using the scoring function on the examples in the pruning set, and the *best* one is selected as the rule learned for the particular seed.

The pruning metric (or scoring function) used is the improved pruning method ν^* as suggested by Cohen[23] and is defined as follows

$$\nu^*(r) = \frac{p(r) - n(r)}{p(r) + n(r)}$$

where $p(r)$ denotes the number of active examples covered by rule r, and $n(r)$ denotes the number of inactive examples covered by r. The ν^* measure is equivalent to precision.[32]

2.4. Implementation. The SMIREP system has been developed in the programming language Python (version 2.3). Python allows rapid prototype development, due to a wide range of available libraries. For SMARTS matching, the open-source chemical library OpenBabel (version 1.100, http://openbabel.sourceforge.net) is employed. All experiments were run on a PC running Suse Linux 9.2 with an Intel Pentium IV-3.2 GHz CPU and 2 GB of main memory. The SMIREP source code is freely available under the GNU General Public License (see section 7 for details).

3. RESULTS

3.1. Validation. Cross-Validation. Tenfold cross-validation was used to evaluate the performance of SMIREP on the three different databases. This means that each complete database was randomly divided into 10 equally sized parts. Each part was once removed from the complete database as a hold out test set, while the remaining other 9 parts were used as a training set for the model. Predictions for the test sets were compared to the actual classifications, to estimate the predictive accuracy. This process was repeated for all 10 parts, so that each part served once as a test set, and predictions for all compounds in the data set are available. As SMIREP's algorithm is heuristic, we repeated the 10-fold cross-validation 10 times to obtain a good estimate of the algorithm's mean accuracy. We call this a 10 × 10-fold cross-validation. In the following sections, we report on the mean predictive accuracies as well as the mean area under ROC curve (see below).

ROC Analysis. A common way to evaluate the performance of a classifier is to employ a confusion matrix. In a confusion matrix the four different possible outcomes (see Table 1) of a single prediction for a two-class problem are displayed in a two-by-two matrix, where the rows represent the number of entries belonging to the actual class, while the columns represent the entries belonging to the predicted class.

Often however, a simple confusion matrix does not properly reflect the classifier's performance. For a more detailed and proper analysis of a classifier, receiver operating characteristics (ROC) curves are employed. ROC curves were first developed for signal detection.[34–37] They are substantially employed in medical tests and have become a standard in the data-mining and machine learning communities to compare different classifiers.

To construct an ROC curve for a classifier, one orders the classifier's predictions by some criterion (typically confidence of a prediction) and then plots the *true positive rate* (defined as TPr = TP/TP+FN) along the *y*-axis against the *false positive rate* (defined as FPr = FP/TN+FP) along the *x*-axis for all possible cutoff values of the criterion values. The resulting curve lies within the unit-square (the ROC space). An ideal ROC curve would be a line along the top left-hand corner (0,1) in ROC space, as it would not produce any false positives (or false actives). In real-world applications this occurs only rarely. The ROC curve for a good prediction should however always be to the left of the diagonal between the two axes. The closer the curve tends toward (0,1), the more accurate are the predictions made.

To compare two different prediction methods, both ROC curves are plotted in the same ROC space. The curve running closer to the left and top border is considered to provide a *better* predictor. Another good measurement to compare ROC curves analysis is that of the *area under the ROC curve* (AUC).[37,38] The AUC gives an overall measure of accuracy of a predictor.

For a more detailed introduction to ROC curves and the construction of ROC curves for rule learner, we refer the reader to Appendix A (Supporting Information).

3.2. Experiments. We evaluated SMIREP on the three databases described in section 2.1. The aim of these experiments was 2-fold: first to demonstrate that activity classification using SMIREP yields accurate rules, and second, to show that meaningful rules can be found, which are sometimes in consensus with the published literature.

Settings. For each of the following experiments, we have chosen arbitrarily the number of seeds such that 10% of compounds classified as active in the database are employed during the growing stage of SMIREP. For example, if the database contain 120 active compounds and 150 inactive ones, we chose the number of seeds to be 12. That means, that SMIREP induces 12 rules for each iteration. To test the effect of different beamsizes, we evaluated SMIREP for each experiment using beamsizes for $k = 5$, 10, and 20. To examine the influence of numerical attributes, we performed two separate experiments, one using only structural information (SAR-setting) and one using the structural information together with logP values and the overall molecular weight of the compounds (QSAR-setting).

DSSTox NCTRER. The database of the 232 chemical compounds from the EPA's DSSTox NCTRER Database was downloaded from http://www.epa.gov/nheerl/dsstox/sdf_nctrer.html. We translated this database to SMILES

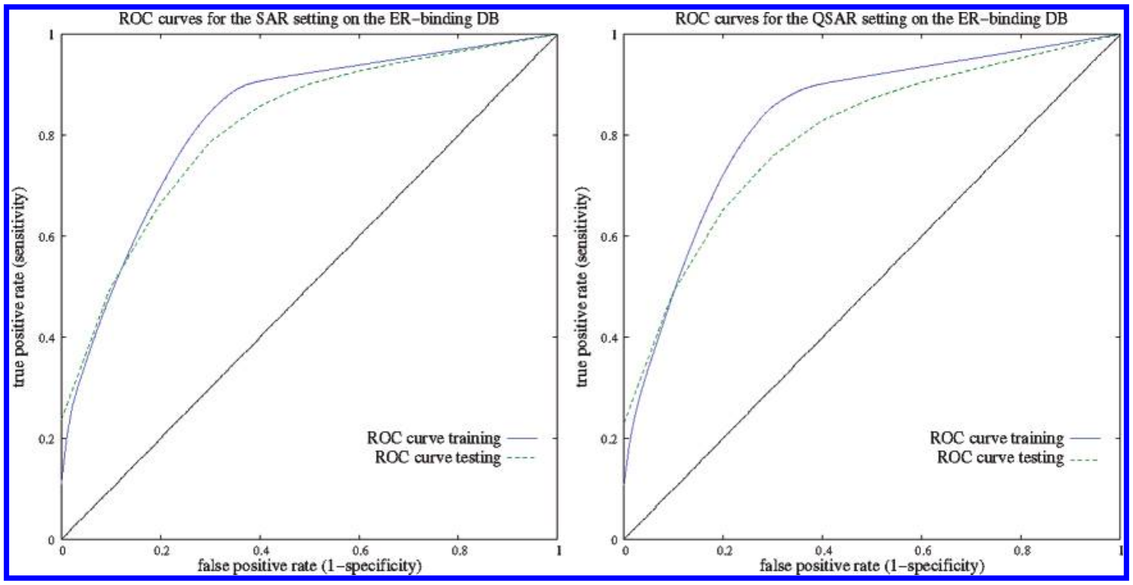

Figure 4. The ROC curves from the SAR and QSAR experiments for training (blue) and testing (green) on predicting the ER-binding database with a beamsize $k = 5$. The ROC curves are averaged over the 10×10 ROC curves resulting from performing ten times a 10-fold cross-validation. The black line indicates the diagonal.

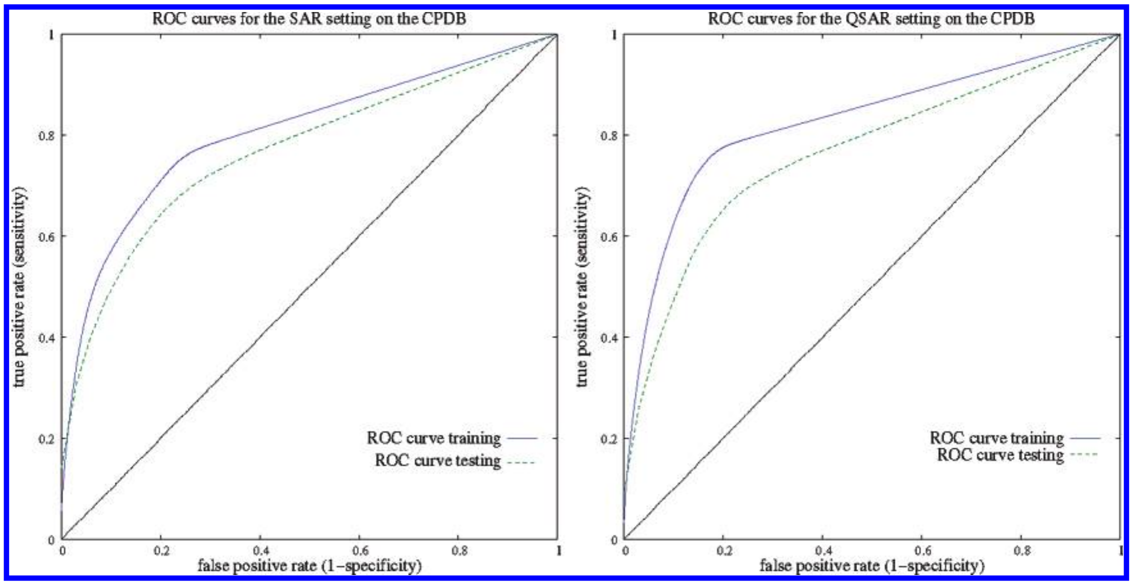

Figure 5. The ROC curves from the SAR and QSAR experiments for training (blue) and testing (green) on predicting the CPDB mutagenicity database with beamsize $k = 5$. The black line indicates the diagonal.

codes using the OpenBabel toolkit. This procedure was necessary, as some SMILES codes provided in the database were corrupt. Furthermore, we removed chiralities (see section 2.2.2) and bond directions from the SMILES strings, as the current version of SMIREP cannot deal with this information. We believe (and the experiments will show) that omitting this information provides SMIREP with enough structure information to induce meaningful and accurate patterns.

The results are depicted in Table 2. Overall, SMIREP seems to perform comparably to the decision tree approach of Hong et al.[39] Although, no specific accuracy is given, Tong et al.[40] report on accuracies of a 3-fold cross-validation experiment resulting roughly in the same prediction accuracies on the training set (approximately 76%, taken from Figure 13.8, p 302). In another recent publication, Hong et al.[41] report on accuracies of 96.6% employing a method called decision forest (DF). DF essentially induces a large number of decision trees and builds a consensus model. In comparison of the original decision tree approach by Hong et al.[39] to SMIREP, no preselection of structural alerts has been performed, as SMIREP is able to extract the relevant information during the learning stage. An example set of rules found during one round of a 10-fold cross-validation is shown in Figure 3.

The computation time varies between the SAR and the quantitative SAR (QSAR) setting. While one complete 10-fold cross-validation using beamsize $k = 5$ averages at around 75 s in the SAR-setting, while SMIREP requires 513 s for a 10-fold cross-validation in the QSAR setting.

Figure 4 depicts the two averaged ROC curves for SMIREP for the SAR setting and the QSAR setting when predicting the ER-binding database for beamsize $k = 5$. The curves represent the averaged 10×10-fold cross-validation results. The averaged area under the ROC curve (AUC) was 0.832 (SAR) and 0.833 (QSAR) for the training sets and

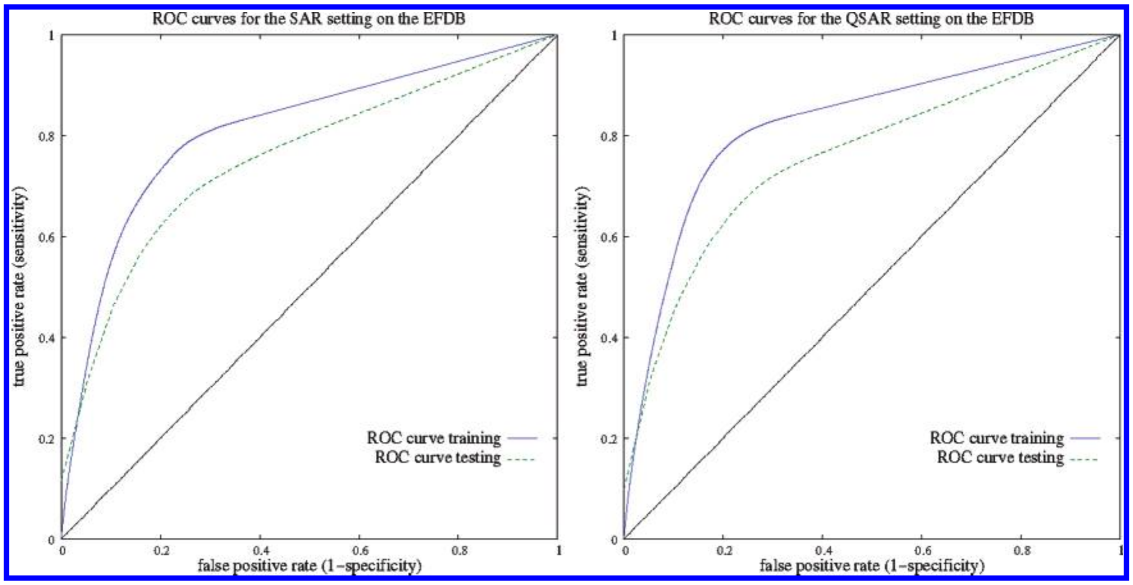

Figure 6. The ROC curves from the SAR and QSAR experiments for training (blue) and testing (green) on predicting the ER-binding database with a beamsize $k = 20$. The ROC curves are averaged over all fold experiments.

0.816 (SAR) and 0.795 (QSAR) for the corresponding test sets. The ROC curves for testing and training are similar, which indicates that SMIREP does not overfit.

As mentioned above, Tong et al.[39] have identified a number of structural features contributing to the ER-binding activity of chemical compounds. Three structural alerts, the steroid skeleton, the steroid diethylstilbestrol (DES) skeleton, and the phenolic ring skeleton, were manually selected as structural alerts, in order to predict the activity class of a potential ER-binding compound. In an earlier publication, Fang et al.[24] have used information about the presence of a ring structure, an aromatic and possibly a phenolic ring structure, and the DES skeleton to build a rule system evaluating the likeliness of a compound being a possible ER ligand. The handcrafted rule system by Fang et al. is as follows:

1. If a chemical contains no ring structure, then it is unlikely to be an ER ligand.

2. If a chemical has a nonaromatic ring structure, then it is unlikely to be an ER ligand if it does not contain an O, S, N, or other heteroatom for bonding. Otherwise its binding potential is dependent on the existence of the key structural features.

3. If a chemical has a non-OH aromatic structure, then its binding potential is dependent on the existence of key structural features (e.g., logP, precise O−O distance, etc.).

4. If a chemical contains a phenolic ring, then it tends to be an ER ligand if it contains any additional key structural features. For the chemical containing a phenolic ring separated from another benzene ring with the number of bridge atoms ranging from none to three, it will be most likely an ER ligand.

The main structural rule in this system is rule number 4, which translates into the following: "if a compound possesses an aromatic ring connected by one to three atoms to a phenolic ring, then the compound is likely to be an ER ligand". We have assessed this rule using the OpenBabel tool *obgrep*. *obgrep* works similar to the UNIX grep command, but instead of using regular expressions it performs a SMARTS search though a database of chemical structures. Overall, this single rule matches 33 of the classified as active compounds, while matching 15 of the non-ER ligands. This however, does not seem to be a very good structural rule when predicting the activity class of unseen compounds. We have compared an example SMIREP rule set with the rule set by Fang et al. This discussion is included in Table 3. Overall, a number of rules correspond to these expert rules.

Table 4. Accuracy and Area under ROC Curve for the CPDB Data Set for Different Beamsizes (k) from the 10 × 10-Fold Cross-Validations[a]

setting	k	acc training	AUC training	acc testing	AUC testing
SAR	5	76.11 (0.28)	0.804 (0.012)	72.87 (1.21)	0.768 (0.056)
	10	75.95 (0.16)	0.801 (0.011)	72.16 (1.05)	0.761 (0.055)
	20	76.07 (0.23)	0.803 (0.010)	72.60 (0.50)	0.765 (0.057)
QSAR	5	79.73 (0.26)	0.825 (0.015)	73.90 (0.99)	0.764 (0.055)
	10	79.61 (0.52)	0.821 (0.016)	74.26 (1.53)	0.766 (0.054)
	20	78.58 (0.44)	0.811 (0.019)	74.20 (1.30)	0.766 (0.040)

[a] The numbers in brackets denote the standard deviation. Increasing the beamsizes in the CPDB experiment does not yield any significant change in the performance of SMIREP.

We believe that this example rule set could aid initially in the construction of an expert rule system for classifying potential ER-binding molecules, like the one presented by Fang et al.[24] Although the discovered rules do not present previously unknown knowledge, they can be used as a first step and guideline for experts.

CPDB. The second data set we evaluated SMIREP on was derived from the carcinogenic potency database (CPDB). The settings used were the default settings described in section 3.2.1. The number of seeds was set to *30*, which corresponds to 10% of compounds classified as active in the training set.

The results are depicted in Table 4. Overall, the predictive performance does not vary as much as in the ER-binding experiment and results also in a lower predictive performance. This might be due to the nature of the application: the CPDB database contains more heterogeneous molecules when compared to the NCTRER database. When comparing these results to the literature, i.e., to the MOLFEA data-

Table 5. Performance of SAR Models for *Salmonella* Mutagenicity Reported in the Literature[7] [a]

author	citation	method	accuracy
Perrotta et al.	42		73.9
Klopman and Rosenkranz	18	CASE	72
Klopman and Rosenkranz	18	MULTICASE	80
Klopman and Rosenkranz	18	CASE/GI	47
Helma et al.	7	MOLFEA/J48	75.5
Helma et al.	7	MOLFEA/PART	75.0
Helma et al.	7	MOLFEA/SMO,E1	76.1
Helma et al.	7	MOLFEA/SMO,E2	73.7

[a] The accuracies for the different MOLFEA approaches were the results on unoptimized structures and averaged overall four different settings.

mining system[7] and to CASE[17] and MULTICASE,[18] this drop in predicted accuracy has to be seen in a different perspective. The results published by Helma[7] and others[18,42] are summarized in Table 5. Although SMIREP achieves similar, though slightly lower, accuracies than the other methods, it is not quite clear whether these differences are statistically significant, as it is not possible to test for statistical significance purely based on accuracies from 10-fold cross experiments without the standard deviations. Therefore, we have calculated a 99% confidence interval for the best result from SMIREP. The accuracy of the best MOLFEA approach (SMO/E1) lies within the interval, indicating that the differences are not statistically significant. In contrast to MOLFEA, however, the produced rules by SMIREP are easy to understand, and SMIREP's ability to employ more complex structures than just linear fragments seems to aid in the rule induction. An example set of rules is presented in Table 6. Some parts of the fragments used in this example rule set were also identified in the MOLFEA approach. However, many of the SMIREP rule sets contain the fragments 'C1OC1' (coding for epoxide, a structure that is often associated with mutagenicity) or more complex fragments like 'c1c2ncccc2ccc1', like in the example rules set in rules 8 and 4, respectively, which can neither be found nor represented using linear fragments.

EFDB. For prediction of the biodegradability in terms of biodegradable or nonbiodegradable, we have used 328 compounds, 185 considered active (biodegradable) and 143 inactive (nondegradable) compounds. As with the other experiments, we evaluated the results in terms of accuracy as well as using ROC analysis. The accuracies are compared to previously published results.

To compare to other published approaches we have modified the evaluation and performed a 5 × 10-fold cross-validation (using the original folds published by Blockeel et al.[27]). We repeated each of these fold-wise experiments arbitrarily five times to allow for a more accurate estimate on the accuracy due to the selection of seeds in SMIREP. We have selected the same folds as Blockeel et al.[27] The results of the SMIREP experiments are depicted in Table 7.

Table 6. Example Rule Set Induced by SMIREP on the CPDB

No	Rules (SMILES)	Rules (2D)
1	nccccnc	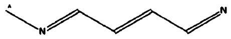
2	N=O	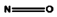
3	cccc ∧ ccN ∧ ccO ∧ OC	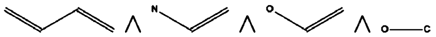
4	c1c2ncccc2ccc1	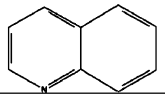
5	CBr	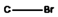
6	CCl ∧ CN	
7	=O ∧ c1occcc1	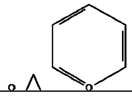
8	C1OC1	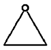
9	c1ccccc1 ∧ Nccc	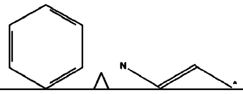
10	N ∧ CCOC	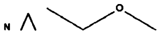
11	NN	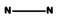
12	c1cc2ccccc2cc1	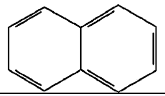

Table 7. Average Accuracies and Areas Under ROC Curve for the EFDB Data Set for a Number of Different Beamsizes (*k*)[a]

setting	*k*	acc training	AUC training	acc testing	AUC testing
	5	77.68 (1.41)	0.811 (0.016)	71.81 (5.61)	0.747 (0.078)
SAR	10	77.05 (1.02)	0.811 (0.015)	71.53 (6.27)	0.756 (0.086)
	20	77.07 (1.18)	0.810 (0.015)	71.65 (6.29)	0.754 (0.084)
	5	79.90 (1.06)	0.826 (0.014)	73.51 (5.08)	0.744 (0.081)
QSAR	10	79.50 (1.25)	0.826 (0.015)	73.14 (5.99)	0.743 (0.079)
	20	79.02 (1.55)	0.822 (0.016)	74.32 (5.83)	0.756 (0.080)

[a] The accuracies of SMIREP in the QSAR setting are comparable to that published by Blockeel et al.[27] when using the *Global* and *R* information.

Table 8. Mean Accuracies on the 5 × 10-Fold Cross-Validation of a Number of Relational Learning Approaches Published by Blockeel et al.[27] Using the *Global* as Well as the Atom/Bond Information (*R*)[a]

method	accuracy
ICL	73.2
Tilde	74.1
S-CART	71.9

[a] The SMIREP QSAR approach performs comparably to these approaches with a mean accuracy on the test data ranging from 73.81% to 74.32% depending on the beamsize *k*.

The performance of SMIREP to other approaches on this data set can be seen in Table 8. Here, we can only compare the accuracies and not the average AUC. In their publication, Blockeel et al.[27] have tested a number of relational learning methods on this data set, with varying background knowledge. The information about the compounds contained in the database is organized into four types of background knowledge: *Global*, *P1*, *P2*, and *R*. The *Global* information reflects global information about a molecule such as the molecular weight and logP. The *R* type encapsulate the atom and bond information, while the types *P1* and *P2* are used as aggregates reflecting information about the frequencies of certain substructures occurring in a given compound (*P2 employs a set of 59 predefined substructures*). We have compared the performance of SMIREP against the algorithms used by Blockeel et al.[27] in the *Global* and *R* type setting, as this is the closest to SMIREP in the QSAR setting. The relational learning approaches tested by Blockeel et al. were not evaluated on the pure atom/bond information R. Comparing the mean accuracies of SMIREP against the ones from Blockeel et al.[27] (in Table 8) shows that SMIREP achieves comparable performance to that of relational learning methods on the classification task.

Although the prediction accuracies of SMIREP when compared to other approaches are quite similar, the performance of SMIREP comes to some extent as a surprise. As SMIREP is neither able to induce rules for both activity classes at the same time nor is—currently—able to incorporate the absence of a fragment within a compound, the good results are hard to explain. However, in the light of this application, these features would very much be required to predict readily degradable compounds and specific half-life times.

4. DISCUSSION

SMIREP is essentially a QSAR based approach able to extract relevant structural fingerprints quickly. Obviously, modeling chemical problems on this level has certain drawbacks. Other approaches in activity prediction employ, for example, the docking site of the protein under consideration. However, in most cases, this information is not or only partially available. And, equally important, these more

Table 9. Example Rule Set Discovered on the EFDB Data Using the QSAR Setting [a]

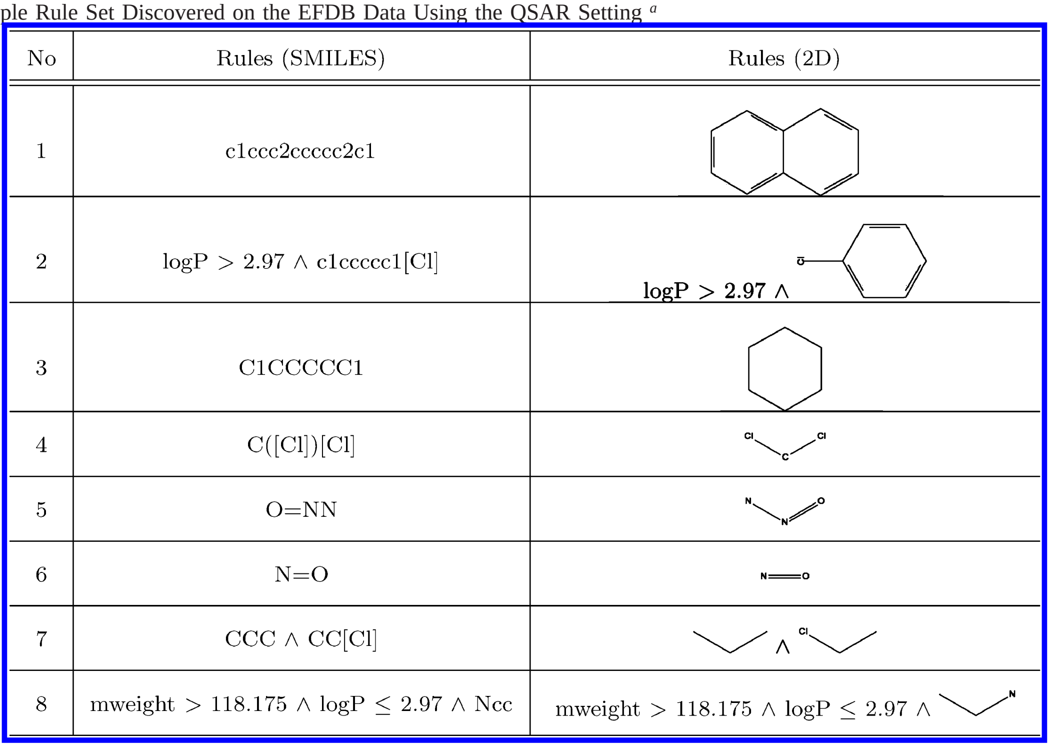

No	Rules (SMILES)	Rules (2D)
1	c1ccc2ccccc2c1	
2	logP > 2.97 ∧ c1ccccc1[Cl]	logP > 2.97 ∧
3	C1CCCCC1	
4	C([Cl])[Cl]	
5	O=NN	
6	N=O	
7	CCC ∧ CC[Cl]	∧
8	mweight > 118.175 ∧ logP ≤ 2.97 ∧ Ncc	mweight > 118.175 ∧ logP ≤ 2.97 ∧

Cl
Cl
C
Cl
N
N
O
N
O
Cl
N

[a] The rules predict nonbiodegradation. The accuracy of this specific rule set is 81.8% (correctly predicting 11 out of 14 examples on the corresponding test set).

sophisticated approaches typically require substantially more computation time.

SMIREP is, to some extent, similar to MULTICASE,[17] in that it constructs fragments based on the structure of chemical compounds and uses these fragments as an integral part of the machine learning approach. However, MULTICASE constructs all possible linear (and to some extent branched) fragments up to a fixed length of 10 non-hydrogen atoms. Using statistical testing, the found fragments are divided into significantly activating fragments (*biophores*) and significantly deactivating fragments (*biophobes*). MULTICASE then automatically defines major biophore classes, and within each class it identifies fragments modifying the overall class activity. These modifying fragments together with calculated numerical attributes, such as logP, octanol–water, charges, densities, etc., are used as so-called *modulators* to refine an activity model of a biophore using a divide-and-conquer search strategy.

The differences between MULTICASE and SMIREP are 3-fold: First, SMIREP does not use biophobes to indicate inhibition (or inactivity), as the use of deactivating fragments is typically not desired within the SAR setting. Second, to avoid overfitting of rules, SMIREP does not employ modulators to fine-tune activities of found biophores. Third, in contrast to MULTICASE, SMIREP is able to employ more complex structures, including rings, and it does not impose a restriction on the overall length of fragments.

The difference of SMIREP with regard to other QSAR approaches can be seen in SMIREP's ability to extract relevant knowledge in the form of structural alerts on during the learning stage. Other approaches rely on precalculated fingerprints, like MDL keys,[1,2] or use physiochemical and structural indeces calculated by specialized software like Molconn-Z.[3] Here, we have presented a system, able to focus on only the important structural features hidden in the database.

In a previous publication,[20] we have compared SMIREP to graph mining approaches which have been employed in SAR. The advantage of SMIREP over most of these systems lies in the small set of rules produced. While approaches such as gSpan, closeGraph,[15] FSG,[5] and AGM[12] typically find a *large* set of patterns satisfying a minimum frequency threshold, which are not necessarily predictive, SMIREP directly builds a *small* set of predictive rules. Furthermore, as these graph based approaches traverse the complete search space of possible patterns, they tend to be inefficient. SMIREP, on the other hand, is a heuristic approach and is able to induce rules faster.

Several improvements are possible for the SMIREP system. As SMIREP employs principle ideas from the machine learning algorithm IREP,[22,23] a next step could be the upgrade of the underlying learning algorithm to some of its successors, for instance RIPPER[23] (Repeated Incremental Pruning to Produce Error Reduction). RIPPER employs the rules found by IREP and repeatedly grows and prunes the found rules to improve the prediction accuracy on different splits for the training and validation sets. Compared to a number of other approaches, SMIREP only induces rules for compounds considered to be active, and no rules are found specifically for inactive compounds. That means that SMIREP has no mechanism to filter out obvious inactive compounds, as done in the decision tree approach by Hong et al.[39] This is clearly a disadvantage when comparing predictive performance. One possible way to overcome this limitation is to employ the fragmentation approach together with a decision tree learner as the underlying learning algorithm or to learn rules for more than one class. For the actual application of SMIREP to SAR, learning rules from active compounds only is less problematic, as one is typically more interested in the understanding of activity rather than inactivity.

In the current implementation, SMIREP does not cater for stereoisomers possessing different activity levels. Indeed, the chirality information is disregarded during learning. However, this information is a major factor when investigating the activity levels of natural compounds. In future versions of SMIREP, we intend to incorporate the chirality information encoded in the compound's SMILES codes into the system.

To accommodate the possibility to incorporate some sort of background or domain knowledge, it is further possible to add predefined structural alerts as new fragments during the growing stage of SMIREP. Although this would be in contrast to the idea of inducing alerts without any prior knowledge, it could overcome some limitations of SMIREP regarding larger ring structures.

5. CONCLUSION

In this paper we have presented a number of applications of a novel system, SMIREP, to predict activity classification in the SAR and QSAR problem setting. SMIREP combines principles of the chemical representation language SMILES with the inductive rule learner IREP. The novelty behind the SMIREP approach is the use of linear strings to induce rules containing complex structures such as trees and cycles. The applicability of SMIREP to classify chemical compounds was demonstrated on three diverse data sets. Overall, the predictive performance of SMIREP is comparable to existing methods. In contrast to other methods,[24,39] there is no need to employ preselected structural alerts or fingerprints for the classification task. Furthermore, as SMIREP is able to induce these alerts ab initio, the found rules can be employed to construct more fine-grained rules sets. We believe, therefore, that SMIREP is a valuable tool to analyze chemical databases.

The SMIREP system is available from http://www.karwath.org/systems/smirep/ under the GNU General Public License. The Web page also contains the data files used in the Experimental Section. The system is provided in Python and C source code, including the required Python OpenBabel module OBGrep.

ACKNOWLEDGMENT

The authors would like to thank Christoph Helma, David P. Enot, Ross D. King, and Siegfried Nijssen for helpful discussions and suggestions. This research was supported by the EU grant FP6-516169 Inductive Querying.

Note Added after ASAP Publication. This article was released ASAP on October 12, 2006 with errors in Table 3, Rule 5. The correct version was posted on October 20, 2006.

Supporting Information Available: Appendix A describing the generation of ROC curves and a more detailed description of ROC analysis. This material is available free of charge via the Internet at http://pubs.acs.org.

REFERENCES AND NOTES

(1) M.D.L. Information Systems, I. 14600 Catalina Street, San Leandro, CA 94577, U.S.A.

(2) Durant, J. L.; Leland, B. A.; Henry, D. R.; Nourse, J. G. Reoptimization of MDL Keys for Use in Drug Discovery. *J. Chem. Inf. Comput. Sci.* **2002**, *42*, 1273−1280.

(3) *Molconn-Z, version 3.50*; available from Hall Associates Consulting, 2 Davis Street, Quincy, MA, 02170. Also available from EduSoft, LC, P.O. Box 1811, Ashland, VA 23005 and SciVision, Inc., 200 Wheeler Road, Burlington, MA 01803.

(4) Dehaspe, L. Frequent Pattern Discovery in First-Order Logic, Thesis, K. U. Leuven: Belgium, 1998.

(5) Deshpande, M.; Kuramochi, M.; Karypis, G. Frequent Sub-Structure-Based Approaches for Classifying Chemical Compounds. In *Proc. ICDM-03*; IEEE Computer Society: Piscataway, NJ, U.S.A., 2003; pp 35−42.

(6) Kramer, S.; De Raedt, L.; Helma, C. Molecular Feature Mining in HIV data. In *Proc. KDD-01*; Provost, F., Srikant, R., Eds.; ACM Press: New York, U.S.A., 2001; pp 136−143.

(7) Helma, C.; Kramer, T.; Kramer, S.; De Raedt, L. Data Mining and Machine Learning Techniques for the Identification of Mutagenicity Inducing Substructures and Structure-Activity Relationships of Noncongeneric Compounds. *J. Chem. Inf. Comput. Sci.* **2004**, *44*, 1402−1411.

(8) Zaki, M. Efficiently Mining Frequent Trees in a Forest. In *Proc. KDD-02*; Hand, D., Keim, D., Ng, R., Eds.; ACM Press: New York, U.S.A., 2002; pp 71−80.

(9) Yan, X.; Han, J. gSpan: Graph-based substructure pattern mining. In *Proc. ICDM-02*; IEEE Press: Piscataway, NJ, U.S.A., 2002; pp 721−724.

(10) Borgelt, C.; Berthold, M. R. Mining Molecular Fragments: Finding Relevant Substructures of Molecules. In *Proc. ICDM-02*; IEEE Press: Piscataway, NJ, U.S.A., 2002; pp 51−58.

(11) Inokuchi, A.; Kashima, H. Mining Significant Pairs of Patterns from Graph Structures with Class Labels. In *Proc. ICDM-03*; IEEE Press: Piscataway, NJ, U.S.A., 2003; pp 83−90.

(12) Inokuchi, A.; Washio, T.; Motoda, H. Complete Mining of Frequent Patterns from Graphs: Mining Graph Data. *Machine Learning* **2003**, *50*, 321−354.

(13) Kuramochi, M.; Karypis, G. Frequent subgraph discovery. In *Proc. ICDM-01*; IEEE Press: Piscataway, NJ, U.S.A., 2001; pp 179−186.

(14) Muggleton, S. Inductive logic programming. *New Generation Computing* **1991**, *8*, 295−318.

(15) Yan, X.; Han, J. CloseGraph: Mining Closed Frequent Graph Patterns. In *Proc. KDD-03*; ACM Press: New York, U.S.A., 2003; pp 286−295.

(16) Kazius, J.; Nijssen, S.; Kok, J.; Bäck, T.; IJzerman, A. P. Substructure Mining Using Elaborate Chemical Representation. *J. Chem. Inf. Model.* **2006**, *46*, 597−605.

(17) Klopman, G. Artificial intelligence approach to structure-activity studies: Computer automated structure evaluation of biological activity of organic molecules. *J. Am. Chem. Soc.* **1984**, *106*, 7315−7320.

(18) Klopman, G. MultiCASE: A hierarchical computer automated structure evaluation program. Quantitative Structure-Activity Relationships. *Quant. Struct.-Act. Relat.* **1992**, *11*, 176−184.

(19) Helma, C. lazar: Lazy Structure-Activity Relationships for Toxicity Prediction. In *Predictive Toxicology*; Helma, C., Ed.; Taylor & Francis: Boca Raton, London, New York, 2005; pp 479−499.

(20) Karwath, A.; De Raedt, L. Predictive Graph Mining. In *Proc. 7th International Conference of Discovery Science, DS 2004*; Suzuki, E., Arikawa, S., Eds.; Springer-Verlag: 2004; Vol. 3245, pp 1−15.

(21) Weininger, D. SMILES, a Chemical Language and Information System 1. Introduction and Encoding Rules. *J. Chem. Inf. Comput. Sci.* **1988**, *28*, 31−36.

(22) Fürnkranz, J.; Widmer, G. Incremental Reduced Error Pruning. In *Proc. ICML 1994;* Cohen, W. W., Hirsh, H., Eds.; Morgan Kaufmann: 1994; pp 70−77.

(23) Cohen, W. W. Fast effective rule induction. In *Proc. ICML 1995*; Morgan Kaufmann: 1995; pp 115−123.

(24) Fang, H.; Tong, W.; Shi, L.; Blair, R.; Perkins, R.; Branham, W.; Hass, B.; Xie, Q.; Dial, S.; Moland, C.; Sheehan, D. Structure−activity relationships for a large diverse set of natural, synthetic, and environmental estrogens. *Chem. Res. Toxicol.* **2001**, *14*, 280−294.

(25) Howard, P.; Boethling, R.; Jarvis, W.; Meylan, W. M.; Michalenko, E. M. *Handbook of Environmental Degredation Rates;* Lewis Publishers Inc.: Chelsea, MD.

(26) Džeroski, S.; Blockeel, H.; Kompare, B.; Kramer, S.; Pfahringer, B.; Laer, W. V. Experiments in Predicting Biodegradability. *Lect. Notes Comput. Sci.* **1999**, *1634*, 80−91.

(27) Blockeel, H.; Džeroski, S.; Kompare, B.; Kramer, S.; Pfahringer, B.; Laer, W. V. Experiments In Predicting Biodegradability. *Appl. Artif. Intelligence* **2004**, *18*, 157−181.

(28) Sayle, R. 1st-class SMARTS patterns, presented at EuroMUG 97, Verona, Italy, 1997. http://www.daylight.com/meetings/emug97/Sayle/ (accessed Dec 13, 2005).

(29) McNaught, A.; Heller, S.; Stein, S. IUPAC- International Chemical Identifier. http://www.iupac.org/projects/2000/2000-025-1-800.html (accessed Mar 3, 2006).

(30) Mitchell, T. *Machine Learning*; McGraw-Hill: Boston, MA, U.S.A., 1997.

(31) Clark, P.; Niblett, T. The CN2 Induction Algorithm. *Machine Learning* **1989**, *3*, 261−283.

(32) Fürnkranz, J.; Flach, P. A. ROC ‘n’ Rule Learning - Towards a Better Understanding of Covering Algorithms. *Machine Learning* **2005**, *58*, 39−77.

(33) Fürnkranz, J. Separate-and-Conquer Rule Learning. *Artif. Intelligence Rev.* **1999**, *13*, 3−54.

(34) Van Trees, H. L. *Detection, Estimation, and Modulation Theory (Part I)*; Wiley: New York, U.S.A., 1968.

(35) Egan, J. P. *Signal Detection Theory and ROC Analysis*; Academic Press: New York, U.S.A., 1975.

(36) Swets, J. A. Measuring the accuracy of diagnostic systems. *Science* **1988**, *240*, 285−293.

(37) Bradley, A. P. The use of the area under the ROC curve in the evaluation of learning algorithms. *Pattern Recognit.* **1997**, *30*, 1145−1159.

(38) Provost, F.; Fawcett, T. Analysis and Visualization of Classifier Performance: Comparison under Imprecise Class and Cost Distributions. In *Proceedings of KDD-97*; Heckerman, D., Mannila, H., Pregibon, D., Eds.; AAAI Press: Menlo Park, CA, U.S.A., 1997; pp 43−48.

(39) Hong, H.; Tong, W.; Fang, H.; Shi, L.; Xie, Q.; Wu, J.; Perkins, R.; Walker, J. D.; Branham, W.; Sheehan, D. M. Prediction of Estrogen Receptor Binding for 58,000 Chemicals Using an Integrated System of a Tree-Based Model with Structural Alerts. *Environ. Health Perspect.* **2002**, *110*, 29−36.

(40) Tong, W.; Fang, H.; Hong, H.; Xie, Q.; Perkins, R.; Sheehan, D.; Receptor-Mediated Toxicity: QSARs for Estrogen Receptor Binding and Priority Setting of Potential Estrogenic Endocrine Disruptors. In *Predicting Chemical Toxicity and Fate*; Cronin, M. T. D., Livingstone, D. J., Eds.; CRC Press: Boca Raton, London, New York, 2004; Chapter 13, pp 285−314.

(41) Tong, W.; Xie, Q.; Hong, H.; Fang, H.; Shi, L.; Perkins, R. Assessment of prediction confidence and domain extrapolation of two structure-activity relationship models for predicting estrogen receptor binding activity. *Toxicogenomics* **2004**, *112*, 1249−125.

(42) Perrotta, A.; Malacarne, D.; Taningher, M.; Pesenti, R.; Paolucci, M.; Parodi, S. A computerized connectivity approach for analyzing the structural basis of mutagenicity in Salmonella and its relationship with rodent carcinogenicity. *Environ. Mol. Mutagen.* **1996**, *28*, 31−50.

CI060159G